Solid-State Electronics Vol. 34, No. 12, pp. 1365–1373, 1991
Printed in Great Britain.

0038-1101/91 \$3.00 + 0.00

ANALYSIS OF I–V MEASUREMENTS ON PtSi–Si SCHOTTKY STRUCTURES IN A WIDE TEMPERATURE RANGE

D. Donoval, M. Barus and M. Zdimal
Microelectronics Department, Slovak Technical University, Ilkovicova 3, 812 19 Bratislava, Czechoslovakia

(Received 22 March 1991; in revised form 22 May 1991)

Abstract—I–V Measurements on PtSi–Si Schottky structures in a wide temperature range from 90 to 350 K were carried out. The contributions of thermionic-emission current and various other current-transport mechanisms were assumed when evaluating the Schottky barrier height Φ_0. Thus the generation–recombination, tunneling and leak currents caused by inhomogeneities and defects at the metal–semiconductor interface were taken into account.

Taking the above-mentioned mechanisms and their temperature dependence into consideration in the Schottky diode model, an outstanding agreement between theory and experiment was achieved in a wide temperature range.

Excluding the secondary current-transport mechanisms from the total current, a more exact value of the thermionic-emission saturation current I_{te} and thus a more accurate value of Φ_b was reached.

The barrier height Φ_b and the modified Richardson constant A^{**} were calculated from the plot of thermionic-emission saturation current I_{te} as a function of temperature too. The proposed method of finding Φ_b is independent of the exact values of the metal–semiconductor contact area A and of the modified Richardson constant A^{**}. This fact can be used for determination of Φ_b in new Schottky structures based on multicomponent semiconductor materials.

Using the experimentally evaluated value $A^{**} = 1.796 \times 10^6\ \mathrm{Am^{-2}\,K^{-2}}$ for the barrier height determination from I–V characteristics the value of $\Phi_b = 0.881 \pm 0.002$ eV was reached independent of temperature.

The more exact value of barrier height Φ_b is a relevant input parameter for Schottky diode computer-aided modeling and simulation, which provided a closer correlation between the experimental and theoretical characteristics.

1. INTRODUCTION

There are many methods of determining the Schottky barrier height Φ_b available involving I–V measurements, C–V measurements and photoelectric measurements as shown by Rhoderick[1] and Sze[2]. For their simplicity I–V measurements are the most popular and commonly used. Like Cohen and Gildenblat[3], we assumed various current-transport mechanisms through the rectifying metal–semiconductor contact when computing the potential barrier height Φ_b.

The method most frequently used in practice preassumes pure thermionic emission *over* the barrier:

$$I_1 = I_{te}\left[\exp\left(\frac{qV}{kT}\right) - 1\right]. \qquad (1)$$

As a refinement of this method the series resistance R_s and the so-called ideality factor n were introduced to include the contributions of other current-transport mechanisms. Then:

$$I = I_{te}\exp\left[\frac{q(V-IR_s)}{nkT}\right]\left\{1 - \exp\left[\frac{q(V-IR_s)}{kT}\right]\right\}, \qquad (2)$$

where

$$I_{te} = AA^{**}T^2\exp\left(\frac{-\Phi_b}{kT}\right), \qquad (3)$$

is referred to as a saturation current. A is the diode area and $A^{**} = 1.12 \times 10^6\ \mathrm{Am^{-2}\,K^{-2}}$ is the modified Richardson constant for an n-type Si (see Andrews and Lepselter[4]).

Equation (2) is commonly used in computing the values of I_{te} and Φ_b providing $n \leqslant 1.1$. As soon as the thermionic emission is no longer the only dominant mechanism or the series resistance R_s is too large the ideality factor n increases. By extrapolating the semilogarithmic plot of I–V relationship its intersection I_{te} with the vertical axis acceptable value when the pure thermionic-emission vanishes and therefore no physical interpretation in calculating Φ_b from (3) is justified.

A different type of external error arises when choosing the linear range from the semilogarithmic I–V relationship plot. The upper limit of the interval is influenced by the series resistance while various other current-transport mechanisms especially for structure with a high barrier height Φ_b push the lower interval limit up, thus reducing the linear region.

This is the reason why several models involving large series resistance and the effects of generation–recombination and leakage currents when determining Φ_b were described by Norde[5], Lien[6] and Donoval *et al.*[7], respectively. It still has remained impossible to fit the experimental I–V curves within a wide range of temperatures employing the models mentioned so far.

2. EXPERIMENT

The Schottky structures in our experiments involved PtSi–Si contacts prepared on n-type epitaxial layers with doping concentration $N_d = 4 \times 10^{21}$ m^{-3}. As a substrate, As-doped wafers were used. To minimize the negative contact edge effects, p-type guard ring structures were created. Square-shaped windows of size 4×4 mm were etched in the SiO_2 layers. Then the Si surface was cleaned by high-frequency sputter etching and *in situ* a 100 nm Pt layer was deposited by high-frequency cathode sputtering. The samples were annealed at 460°C in vacuum with an ambient pressure of about 10^{-3} Pa. Then they were introduced into the liquid nitrogen cryostat. Some of the I–V characteristics measured at various temperatures are shown in Fig. 1. In the temperature range from 90 up to 350 K approx. 40 I–V relationships were measured allowing us to plot I–T relationships for various forward biases applied as shown in Fig. 2.

3. DISCUSSION

The barrier height Φ_b calculated from (2) and (3) tends to go down towards lower temperatures since it dropped from $\Phi_b = 0.85$ eV at 350 K to $\Phi_b = 0.54$ at 90 K as one can see in Fig. 3 while, at the same time, the ideality factor rose from $n = 1.08$ to $n = 1.92$ (Fig. 4). This fact might be evidence that, at a first glimpse, the generation–recombination contribution to the total current becomes more significant. The generation–recombination current can be described by the relation:

$$I_2 = I_{gr}\left\{\exp\left[\frac{q(V-IR_s)}{2kT}\right] - 1\right\}, \tag{4}$$

where

$$I_{gr} = \frac{qn_i w}{2\tau}. \tag{5}$$

Here w is the thickness of the semiconductor depletion region, τ is the electron effective lifetime within the depletion region and n_i is the intrinsic electron concentration.

Let us assume a temperature-independent thickness of the depletion region w and a temperature-

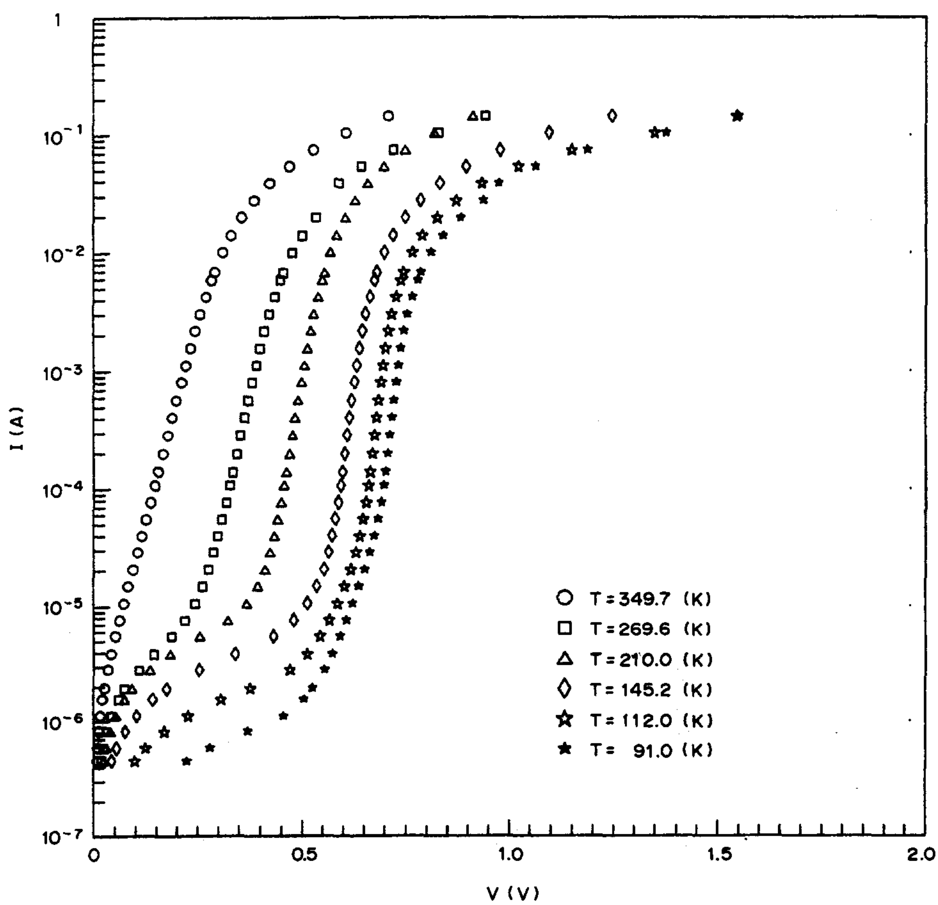

Fig. 1. Forward I–V characteristics of PtSi–Si structures measured in a wide temperature range.

independent lifetime τ. Then the energy gap E_g can be found from the plot of I_{gr} as a function of temperature using:

$$n_i = (N_c N_v)^{1/2} \exp\left(-\frac{E_g}{2kT}\right), \quad (6)$$

where

$$N_c = 2\left(\frac{2\pi m_c^* kT}{h^2}\right)^{3/2}$$

$$N_v = 2\left(\frac{2\pi m_v^* kT}{h^2}\right)^{3/2},$$

are the effective densities of states in the conduction and valence band of the semiconductor, respectively, and m_c^* and m_v^* are the corresponding effective masses of electrons and holes.

Plots of I–T relationships for various forward biases shown in Fig. 2 can be fitted by two straight lines. In the higher temperature region under the assumption of dominant thermionic emission, the following results can be presented: the barrier height varied from $\Phi_b = 0.685$ eV at forward bias $V_a = 0.1$ V to $\Phi_b = 0.820$ eV at $V_a = 0.5$ V. In the lower temperature region, with the generation–recombination process as the dominant one, the energy gaps evaluated were $E_g = 0.185$ eV at $V_a = 0.1$ V and $E_g = 0.577$ eV at $V_a = 0.5$ V. It is obvious when comparing these values with the true PtSi–Si Schottky diodes barrier height $\Phi_b \cong 0.85$ eV and Si energy gap $E_g = 1.12$ eV, respectively, that incorrect results can result when one is applying the above-mentioned assumptions and additional current-transport mechanisms contribute to the total current.

It follows from the herein given analysis that it is necessary to take into account the tunneling current *through* the barrier given by:

$$I_3 = I_t\left\{\exp\left[\frac{q(V-IR_s)}{E_0}\right] - 1\right\}, \quad (7)$$

with I_t as a tunneling saturation current and E_0 as the parameter dependent on the barrier transparency and the so-called leakage current expressed as:

$$I_4 = \frac{V-IR_s}{R_l}, \quad (8)$$

where the resistance denoted as R_l limits the ohmic part of the leakage current and represents the inhomogeneities and defects at a biased metal–semiconductor interface. The equivalent circuit of the Schottky structure is shown in Fig. 5.

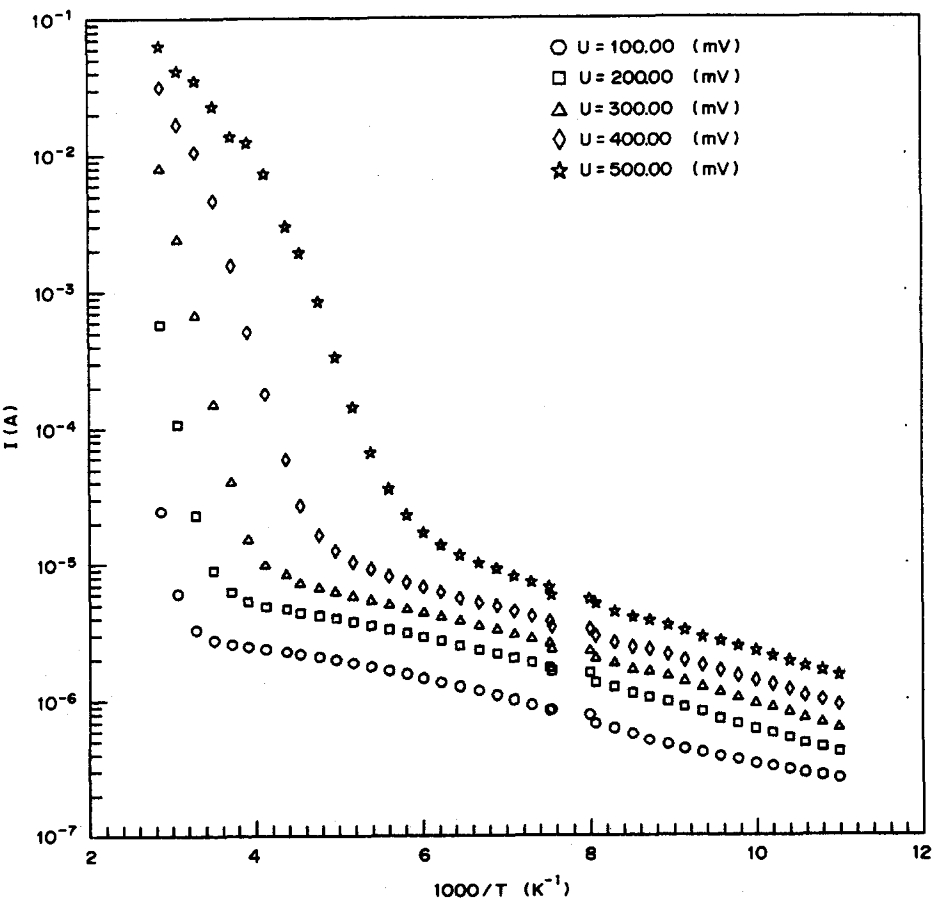

Fig. 2. Temperature dependence of forward current for different applied voltages.

The resistances R_{te}, R_{gr}, R_t and R_l were introduced to represent different current-transport mechanisms through the structure. Then for the total current:

$$I = \sum_{i=1}^{4} I_i = I_{te}\left\{\exp\left[\frac{q(V-IR_s)}{kT}\right]-1\right\} + I_{gr}\left\{\exp\left[\frac{q(V-IR_s)}{2kT}\right]-1\right\} + I_t\left\{\exp\left[\frac{q(V-IR_s)}{E_0}\right]-1\right\} + \frac{V-IR_s}{R_l}. \quad (9)$$

Choosing the proper saturation currents I_{te}, I_{gr}, I_t, the tunneling parameter E_0 and the resistances R_s and R_l allows us to fit the experimental I–V plots in a wide range of applied biases and at various temperatures. The change of temperature results in the change of contribution of individual current-transport mechanisms to the total current. At higher temperatures the thermionic-emission and the generation–recombination are dominant while the tunneling current and leakage current become more significant at lower temperatures. In our case, the tunneling current was no longer negligible at temperatures below 180 K. On the other hand, the generation–recombination current allows for a tighter fit of experimentally achieved data at temperatures above 170 K or so. Below this temperature, it has no significant influence on the fit of experimental characteristics.

Figure 6 shows the effect of the generation–recombination current on the final relationship. The parameters chosen for a data fit at 210 K were $I_{te} = 8.8 \times 10^{-16}$ A, $I_{gr} = 3.78 \times 10^{-12}$ A, $R_l = 4.75 \times 10^4\ \Omega$ and $R_s = 2.85\ \Omega$. A satisfactory fit was achieved as shown in Fig. 6a. At this temperature the tunneling current has no influence on the total current. Neglecting the generation–recombination current by setting $I_{gr} \equiv 0$ would result in a significant discrepancy between the experimental data and the theoretical curves in their breaking region (Fig. 6b).

The effect of the tunneling current on experimental curves is demonstrated in Fig. 7. At 104.6 K an outstanding fit was achieved using parameters $I_{te} = 1.1 \times 10^{-37}$ A, $I_{gr} = 4.86 \times 10^{-26}$ A (I_{gr} is not relevant here), $I_t = 6 \times 10^{-12}$ A, $E_0 = 42.4$ meV, $R_l = 2.685 \times 10^5\ \Omega$ and $R_s = 5.2\ \Omega$ as shown in Fig. 7a. Again similar deviation from the experimental plot occurs when neglecting the tunneling current by setting $I_t \equiv 0$ as one can see in Fig. 7b.

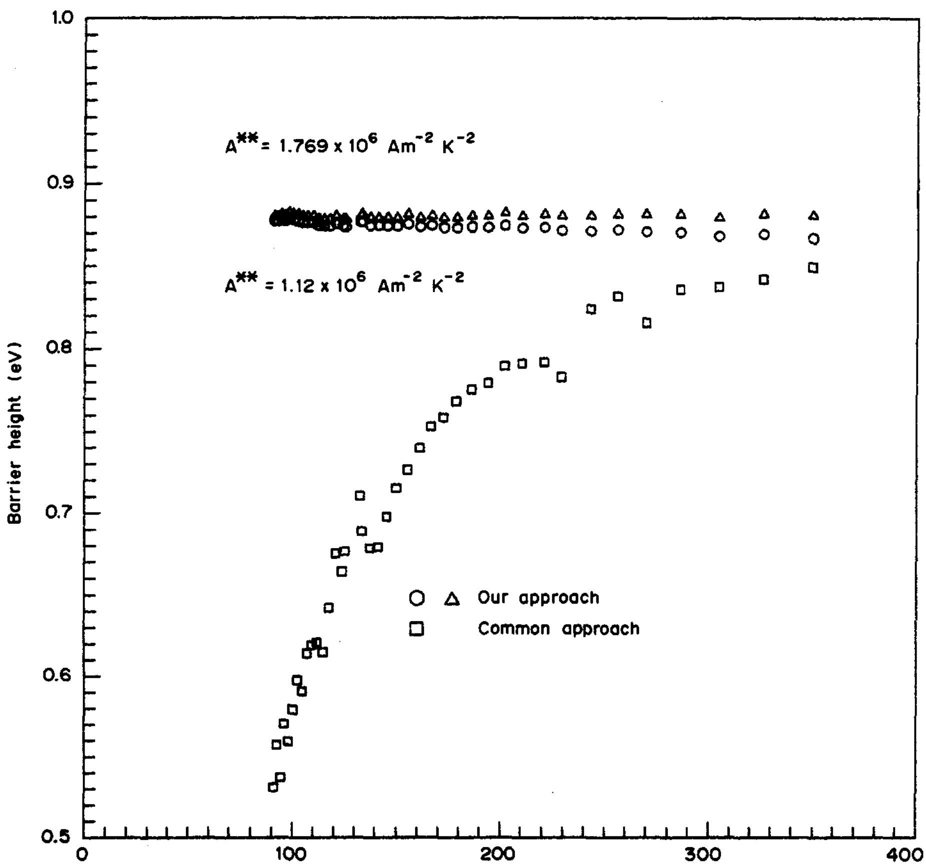

Fig. 3. Temperature dependence of barrier height Φ_b determined by: □, common approach; ○, our approach.

The described model is well-applicable for fitting of I–V characteristics in a wide temperature range and enables us to determine the saturation currents I_{te}, I_{gr} and I_t. Figure 8 shows an experimental plot of I_{te}/T^2 vs $1/T$ which can easily be substituted by a straight line. From this line, by applying eqn (3), we get $\Phi_b = 0.881$ eV and $A^{**} = 1.796 \times 10^6\ \mathrm{Am^{-2}\ K^{-2}}$. Introducing this experimentally-evaluated value A^{**} for PtSi–Si structures into eqn (3) for barrier height determination from I–V characteristics we reached a value of $\Phi_b = 0.881 \pm 0.002$ eV, which matches closely with the value of Φ_b determined by the proposed procedure from the activation energy plot within an experimental error. In such a case the temperature dependence of Φ_b vanishes (see Fig. 3) and we can say that the barrier height Φ_b is independent of temperature. In Fig. 3, we can see also the very slight temperature dependence of Φ_b evaluated in the same way with $A^{**} = 1.12 \times 10^6\ \mathrm{Am^{-2}\ K^{-2}}$.

Figure 9 shows a plot of $I_{gr}/T^{3/2}$ vs $1/T$ with experimentally relevant data at temperatures above 170 K. From the linear fit the energy gap $E_g = 1.11$ eV was calculated using (5) and (6), which corresponds to tabulated $E_g = 1.12$ eV for Si.

The results obtained from the relationships of I_{te} and I_{gr} as a function of temperature have proved the choice of the model allowing us to separate the effect of particular current-transport mechanisms from the thermionic-emission and to reach a more accurate value of Φ_b. In support of this conclusion the relationships of I_t and E_0 as functions of temperature shown in Figs 10 and 11, respectively, can be used. Padovani and Stratton[8] give the tunneling current parameter E_0 as:

$$E_0 = E_{00} \coth\left(\frac{E_{00}}{kT}\right). \tag{10}$$

The dashed line in Fig. 11 is plotted employing relationship (10) under the assumption $E_{00} = 42.2$ meV. Similar tunneling current behavior was observed by Padovani and Stratton.

The values of R_s and R_l are shown in Figs 12 and 13 in terms of their temperature dependence. In both cases an abrupt increase of resistivity at low temperatures can be seen which can be due to the lack of free charge carriers as a result of imperfectly ionized impurities at low temperatures. Assuming that R_l is inversely proportional to the free electron concentration n, at low temperatures one can write:

$$n = \left(\frac{N_d N_d}{2}\right)^{1/2} \exp\left(-\frac{\Delta E_d}{2kT}\right) \tag{11}$$

and the donor activation energy could be determined. Then from the $R_l = f(T)$ relationship for temperatures under 100 K we get the value $\Delta E_d = 0.065$ eV. According to the fact that we neglect the temperature dependence of mobility which could be rather complicated, the evaluated value of ΔE_d corresponds very well with $\Delta E_d = 0.044$ eV for P impurities in Si[9]. This fact can be used as indirect evidence for our previous assumption about the ohmic character of leakage current, too.

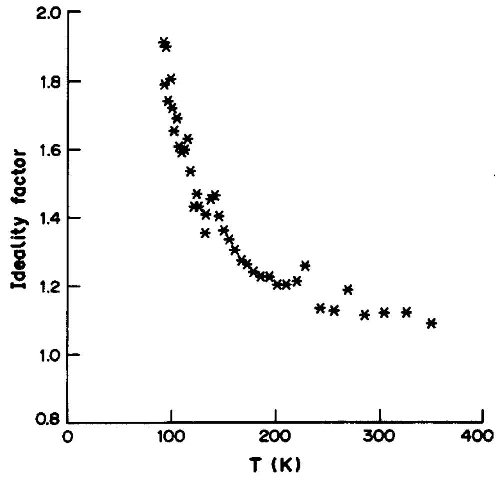

Fig. 4. Temperature dependence of ideality factor n determined by the common approach.

It can be seen from the relationships in Figs 8–13 that I_{te} and R_l are the most exactly determined parameters. It is a matter of fact that the leakage current characterized by the resistance R_l plays a more important role at lower biases while the thermionic-emission current gets dominant in the resulting relationships at higher biases. On the other hand, to find the acceptable values of I_{gr} and particularly I_t which strongly affect the shape of the relationships in the region where neither of the two previous mechanisms is dominant can be a severe limitation.

4. CONCLUSIONS

For several examples we presented a method which brings out the contributions of different current-transport mechanisms to the total current flowing through a forward-biased Schottky structure. The agreement between theory and experiment and the results achieved from the relationships of I_{te} and I_{gr} as functions of temperature justify the proposed model. In this paper we also point out the temperature ranges where individual mechanisms of current flow play dominant roles in the resulting I–V characteristics.

The outlined method allows us to assess the effect of particular mechanisms on the total current and

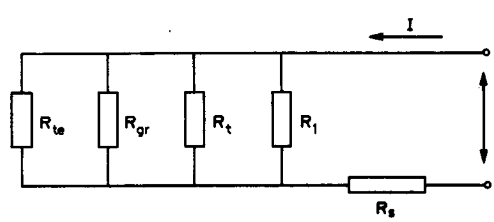

Fig. 5. Proposed d.c. equivalent circuit of Schottky structure.

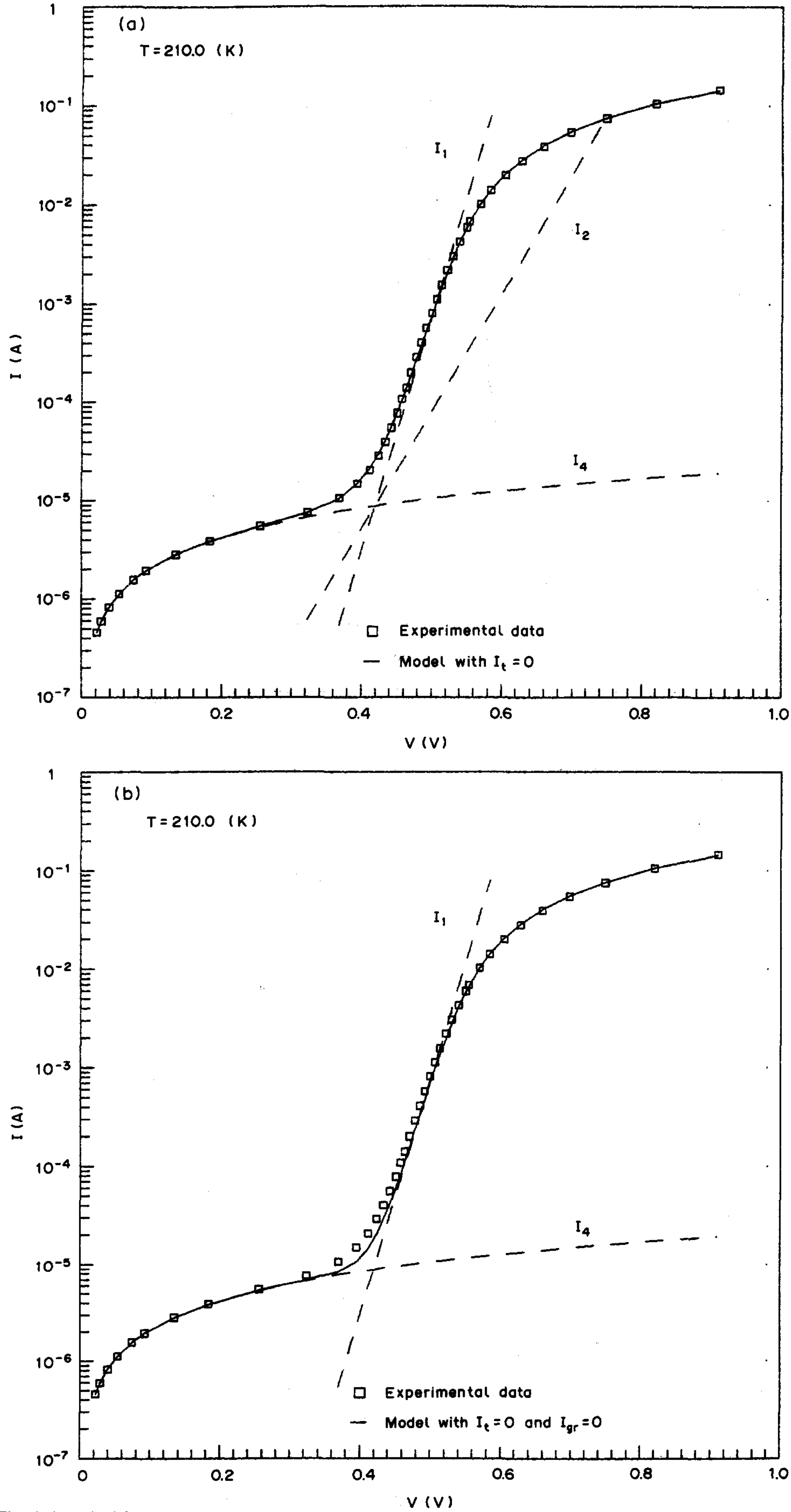

Fig. 6. A typical fit of experimental data for higher temperatures above 170 K by our model with: (a) $I_t = 0$; and (b) $I_t = 0$, $I_{gr} = 0$.

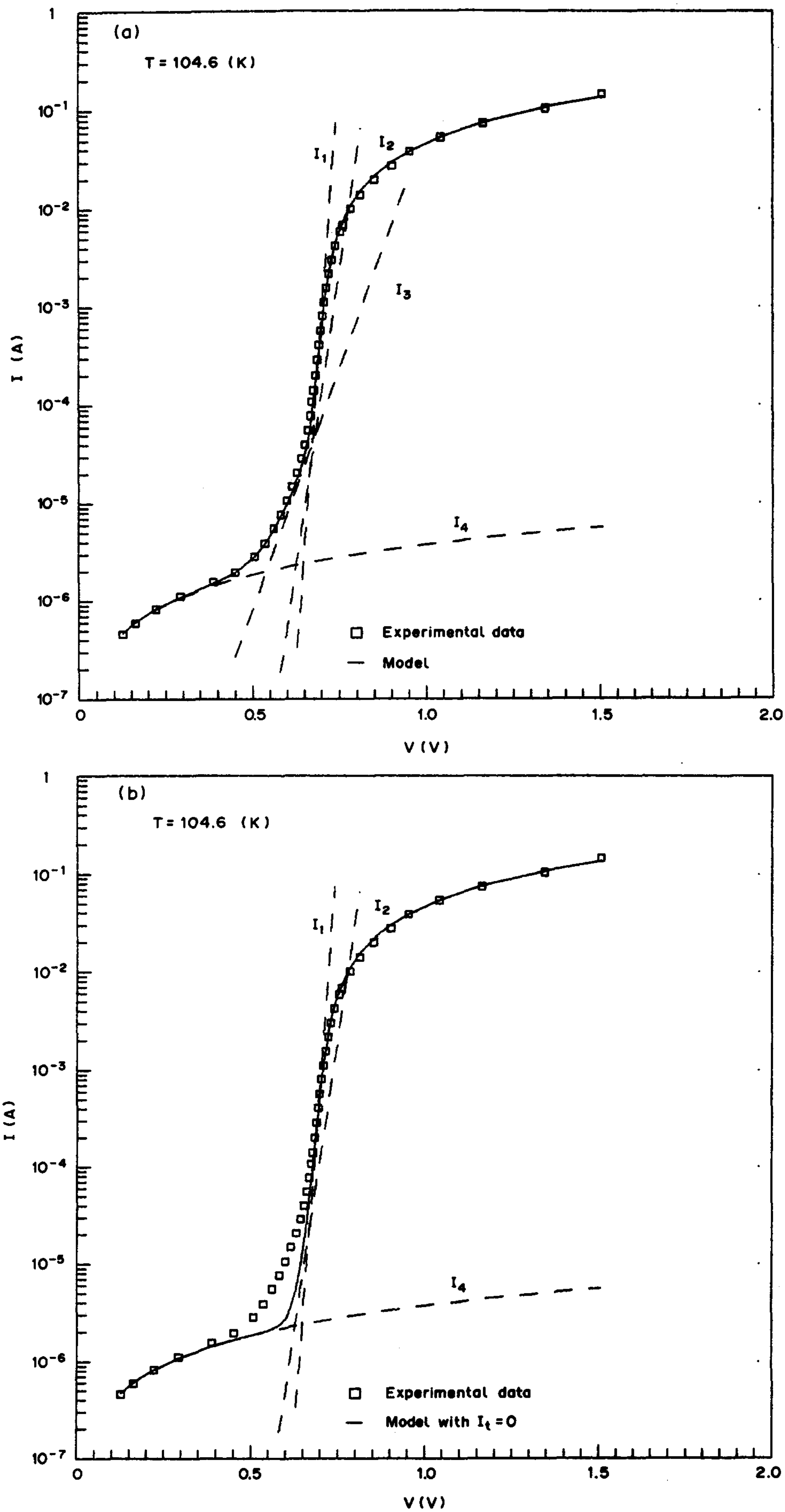

Fig. 7. A typical fit of experimental data for low temperatures by our model with: (a) all components; and (b) $I_t = 0$.

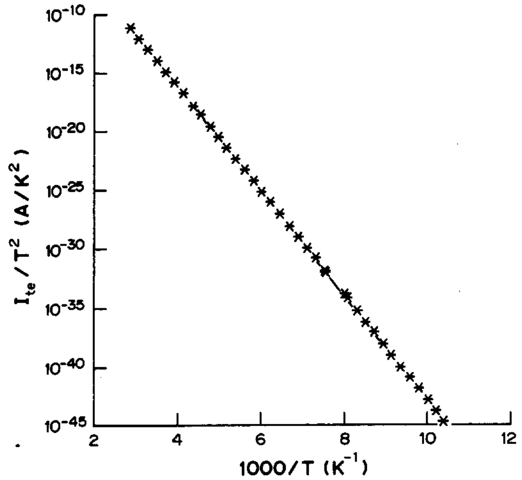

Fig. 8. Temperature dependence of thermionic-emission current I_{te}.

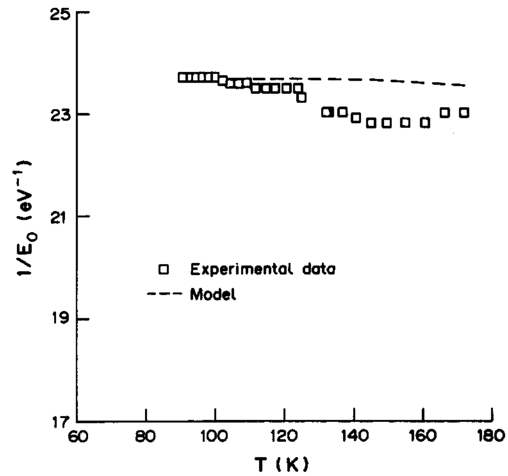

Fig. 11. Temperature of tunneling parameter E_0.

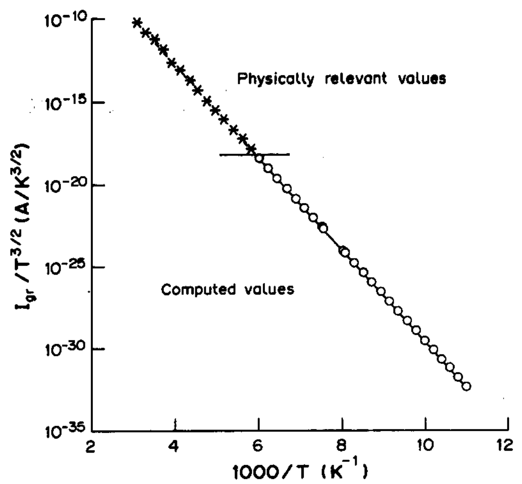

Fig. 9. Temperature dependence of generation–recombination current I_{gr}.

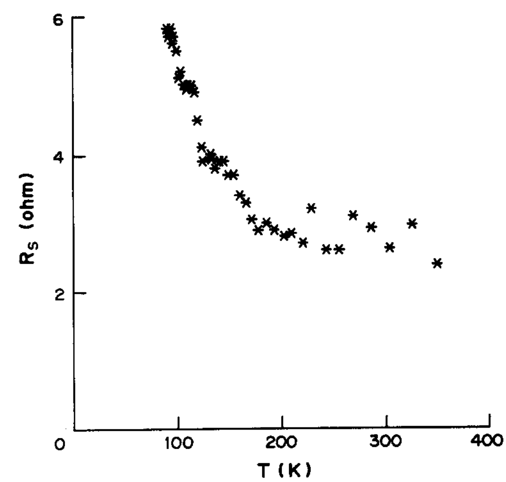

Fig. 12. Temperature dependence of series resistance R_s.

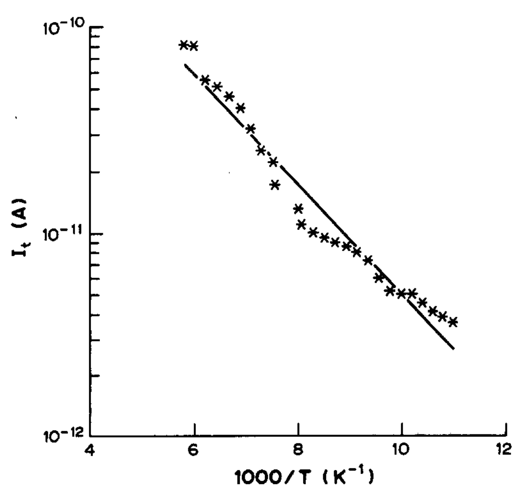

Fig. 10. Temperature dependence of tunneling saturation current I_t.

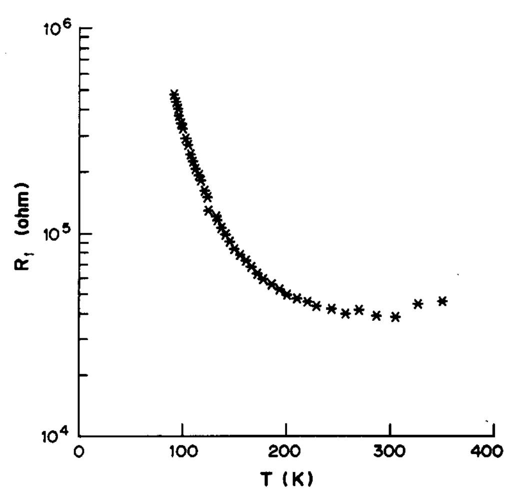

Fig. 13. Temperature dependence of leakage resistance R_l.

to determine the thermionic-emission current more exactly at various temperatures. From the plot of I_{te}/T^2 vs $1/T$ the barrier height was calculated even though the contact area A and the modified Richardson constant A^{**} remain unknown. This routine can be used especially in the new-type Schottky diodes (e.g. on multi-component semiconductor materials) analysis when the exact value of the Richardson constant is not available. Moreover, A^{**} can be found from the appropriate plot. Using an experimental value of A^{**} for our PtSi–Si structure, we found the barrier height Φ_b to be independent of temperature.

The proposed method permits the evaluation of the barrier height even in the case when the linear section of the semilogarithmic I–V plot is affected by various inhomogeneities and defects causing leaks in its lower part and by large series resistance in its upper part. Furthermore, our analysis is based on pure physical knowledge and no artificial functions were introduced as was the case in the papers of Norde or Lien.

We also would like to point to the fact that direct calculations of the barrier height from experimental I–V and I–T characteristics do not have to be absolutely correct, in particular when there are more current-transport mechanisms present in a given temperature interval. The results of the analysis of individual current-transport mechanisms can be useful in diagnostics of the Schottky diodes manufacturing process. A large leakage current or an increased generation–recombination current give evidence of the presence of a considerable amount of defects at the interface and signalize the necessity to revise the technological process.

An exact value of barrier height Φ_b is an important input parameter for computer-aided modeling and simulation of Schottky structure characteristics for better agreement between the experimental data and simulated results. In the present method we calculate a more exact value of the barrier height separating the thermionic-emission current from the total current in a wide range of temperatures.

A question arises whether or not to strive to find a physical interpretation of the change of ideality factor with temperature. The ideality factor was shown to be extremely dependent on the contributions of particular current-transport mechanisms to the total current; the ratio of which to the thermionic-emission current changes with temperature.

In the long run, we would like to mention the case when a dielectric interface layer is present or on electric dipole layer exists at the interface. Then one must take into account other effects contributing to the total current at a given bias to reach a better agreement between theory and experiment.

REFERENCES

1. E. H. Rhoderick, *Metal–Semiconductor Contacts*. Clarendon Press, Oxford (1978).
2. S. M. Sze, *Physics of Semiconductor Devices*, 2nd Edn. Wiley, New York (1981).
3. S. S. Cohen and G. Sh. Gildenblat. *Metal–Semiconductor Contacts and Devices*. Academic Press, London (1986).
4. J. M. Andrews and M. P. Lepselter, *Solid-St. Electron.* **13,** 1011 (1970).
5. H. Norde, *J. appl. Phys.* **50,** 5052 (1979).
6. C. D. Lien, F. C. T. So and M. A. Nicolet, *IEEE Trans. Electron Devices* **ED-31,** 1502 (1984).
7. D. Donoval, J. De Sousa Pires, P. A. Tove and R. Harman, *Solid-St. Electron.* **32,** 961 (1989).
8. F. A. Padovani and R. Stratton, *Solid-St. Electron.* **9,** 695 (1966).
9. S. Wang, *Fundamentals of Semiconductor Theory and Device Physics*. Prentice-Hall, Englewood Cliffs, NJ (1989).